Vibrational dynamics in solid α-oxygen: Experimental assessment of spin-phonon couplings

A. de Bernabé, G. J. Cuello, and F. J. Bermejo
Consejo Superior de Investigaciones Científicas, Serrano 123, Madrid E-28006, Spain

F. R. Trouw
Argonne National Laboratory, Argonne, Illinois 60439-4815

A. P. J. Jansen
Laboratory of Inorganic Chemistry and Catalysis, Eindhoven University of Technology, 5600 MB Eindhoven, The Netherlands
(Received 19 December 1997; revised manuscript received 1 July 1998)

The dynamics of α-oxygen is investigated by means of high-resolution inelastic neutron scattering. The generalized frequency distribution for vibrational motions is derived from the large-angle spectra. A comparison of spectra on both sides of the $\alpha \rightarrow \beta$ magnetic ordering transition provides a clear indication of the extent of the coupling between the magnetic and lattice degrees of freedom. The specific heat and vibrational mean-square amplitudes are calculated from the spectra and compared with experimental and *ab initio* results. The latter also aids with the assignment of the spectral features, and to reconcile the present observations with previous measurements. [S0163-1829(98)07045-3]

I. INTRODUCTION

Despite being the simplest nonmetallic magnet and the only known single-element insulator which is an antiferromagnet, a self-consistent picture of the magnetic dynamical properties of solid α-oxygen is still not available. This situation persists eight decades after the first reported studies on the magnetic properties of the condensed phases of molecular oxygen.[1] At ambient pressure, oxygen can be condensed into a paramagnetic liquid phase 54.4 K$\leqslant T \leqslant$88 K which transforms upon subsequent cooling into a rotator crystal 43.8 K$\leqslant T \leqslant$54.4 K which, as far as the magnetic susceptibility is concerned, also behaves as a paramagnet. Two orientationally ordered phases are known to exist in the temperature ranges 23.9 K$\leqslant T \leqslant$43.8 K (β-O_2, rhombohedral $m\bar{3}m$) and below 23.9 K (α-O_2, monoclinic $c2/m$). From the macroscopic magnetic susceptibilities[2,3] the presence of antiferro(AF)-magnetic-long-range-order (MLRO) in the lowest temperature phase was inferred. The crystal into which the α phase transforms above 23.9 K, known as the β phase, shows a susceptibility which also increases with increasing temperature, suggestive of antiferromagnetic behavior. However, neutron diffraction studies[4] revealed Bragg reflections of magnetic origin only within the α phase. These are compatible with a two-sublattice antiferromagnet structure with moments of about $1.4\mu_B$,[5] which may either be parallel to the monoclinic *b* axis (see inset in Fig. 1) or show some degree of canting, possibly of dynamic origin, within the monoclinic *a*-*b* planes. Such reflections transform into a broad component of diffuse origin[4,5] when the $\alpha \rightarrow \beta$ transition is crossed from the α phase.[6]

Specific heat and thermal conductivity data[7,8] reveal a λ-type anomaly at the $\alpha \rightarrow \beta$ transition, concomitant with a substantial drop in the thermal conductivity.[8,9] The character of such transition (which is driven by magnetoelastic coupling[6]), is now accepted to be of first order, after recent measurements which demonstrated latent heat and hysteresis effects.[10] The transition results in slight modifications of the crystal structures, which are related by a modest lattice distortion of the hexagonal basal plane of β-O_2,[11,12] comprising a small contraction in the **a** direction and a concomitant dilation in the **b** direction.

As regards the spin-dynamics of the low temperature solid, most results have been derived from optical spectroscopies,[13] which sample the $Q \rightarrow 0$ spectrum and provide information on the antiferromagnetic-resonance (AFMR) frequencies. Two AF-spin-wave modes are sustained by α-O_2 (Ref. 14) which correspond to a spin configuration (see inset of Fig. 1) where the magnetic moments are confined within the monoclinic *a*-*b* plane, each one being surrounded by four nearest neighbors on the opposite magnetic sublattice and by two next-nearest neighbors of the

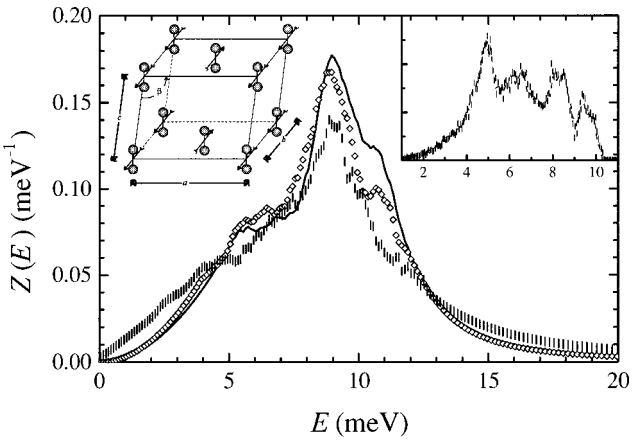

FIG. 1. Estimates for the $Z(E)$ vibrational densities of states for α oxygen at $T=4$ K (solid line), $T=23$ K (diamonds), and β-O_2 at $T=25$ K (vertical bars). The inset at the upper left corner depicts the lattice and magnetic structures of α oxygen. That on the upper right shows the frequency spectra as calculated from harmonic lattice-dynamics procedures (see text) for the α (line) and β crystals (vertical bars).

same sublattice. Adjacent planes are such that the nearest neighbors also belong to the opposite sublattice. To describe the magnetic system, a phenomenological spin-Hamiltonian such as[15,16]

$$H=-2\sum_{ij} J_{ij}\mathbf{S}_i\cdot\mathbf{S}_j+\sum_i [-DS_{xi}^2-D'S_{yi}^2+D'S_{zi}^2] \quad (1)$$

is often used. Here x and z stand for the average spin (preferred magnetization) and molecular axis, respectively. The first sum runs over ij sites having a well defined magnetic moment and J_{ij} represents the Heisenberg exchange coupling between the $^3\Sigma_g^-$ triplet O_2 molecules within their ground states. Such coupling is known to be highly anisotropic,[17] showing remarkably strong dependence on both intermolecular separation and relative orientation of the molecules. To specify in full such a Hamiltonian, a minimum set of J_{ij} exchange constants are needed. In most treatments of experimental data, the dependence on intermolecular distance and relative orientation is modeled by a suitably adjusted set of values. The coupling a of given spin to the four in-plane nearest neighbors (within the crystal a-b plane) will be termed J_{NN}, whereas J_{NNN} represents the intra-sublattice interaction within the plane, and $J_\perp$ for interactions with neighbors in opposite planes. Setting the axes so that the x and z are directed along the main spin direction (crystal b axis) and the direction of the molecular bonds respectively, two additional constants D,D' are needed to specify the two anisotropy terms. Bounds on the magnitudes of the anisotropy constants are given by the free-molecule value, which sets $D+D'=0.5$ meV,[18] and from the experimental values of the AFMR frequencies which are given by

$$(1+\delta\langle S\rangle_0)[-16(J_{NN}-J_\perp)(D\pm D')]^{1/2}, \quad (2)$$

where $\delta\langle S\rangle_0$ stands for the zero point spin deviation (a value of 0.2 corresponds to a quadratic layer with $r=4$ neighbors).

The values for the other required constants, particularly the ratio $J_\perp/J_{NN}$ which reflects the relative strength of interplanar couplings,[19,20] are still a matter of debate. Some constraints linking different J's can be found in the literature, mostly as a result of magnetic susceptibility measurements,[2,3,16] but the small number of independent observations has hindered attempts to develop a consensus on the values for these parameters. Indeed, parameter sets as different as $J_{NN}=-3.32(-2.44)$ meV, $J_{NNN}=-0.91$ (-1.22) meV, $J_\perp<0(0)$ meV have been reported from spectroscopic experiments, and even greater discrepancies were found concerning the anisotropy constants.

The only reported inelastic polarized neutron scattering experiment[16] describes a unique feature at $\approx$10 meV and $Q=1.3$ Å^{-1} (resolution limited in both, energy and momentum transfers) appearing in the spin-flip channel. The study implied that the magnetic couplings are predominantly bidimensional (i.e., $J_\perp=0$ meV). The signal was assigned to a $(0,\frac{1}{2},0)$ zone-boundary AF magnon on the basis of a model for the magnon density of states, which was chosen to be consistent with the constraint imposed by the two AFMR frequencies. No signatures of any other AF spin wave were seen in the experiment.

A question which does not seem to have been addressed, at least on semiquantitative grounds, is the extent in frequency and the strength of the coupling between the molecular and spin degrees of freedom. Some estimates have been given on the basis of limited experimental data[16] or from quantum-chemical calculations.[21] The difficulty in assessing the importance of such coupling arises from the lack of reliable data regarding basic quantities, such as the vibrational frequency distribution (density of states). The vibrational spectra for both α and β oxygen have been calculated several times,[22,23] but such results have not been compared with experiment. Since the experimental spectra were not available from previous neutron measurements,[16] a first measurement of the low-frequency part of the vibrational spectrum was carried out using unpolarized neutrons and a high energy-transfer resolution.[25] The powder averaged $\langle S(Q,E)\rangle$ was analyzed for wavevectors either close to, or far from a magnetic Bragg reflection. This approach, in conjunction with spectra for the β phase, highlighted the magnetic nature of a feature which appeared at about 4.5 meV, superimposed on a relatively broad phonon wing. The experiment was limited by neutron kinematics, which hindered the exploration of frequencies above 6 meV. To overcome this limitation, a new set of measurements has been carried out. The two main aims of these new experiments was to obtain the frequency distribution for vibrational motions for the two low-temperature phases of oxygen (long overdue), and to compare the spectrum at temperatures above and below the $\alpha\rightarrow\beta$ magnetic ordering transition, to explore the changes in the lattice dynamics concomitant with the presence of MLRO.

II. EXPERIMENTAL DETAILS

The data reported here correspond to measurements carried out on the QENS instrument[24] at the Intense Pulsed Neutron Source located at the Argonne National Laboratory. The instrument provides coverage of a wide range of energy-transfers while retaining a good energy-resolution, $\Delta E\approx 90$ μeV [full width at half maximum (FWHM)] at zero energy transfer. QENS is an inverted-geometry crystal-analyzer spectrometer looking at a solid methane moderator, and operates with fixed final energy $E_f=3.65$ meV. The incident neutron spectrum covers a wide range of energies (a ''white'' neutron spectrum) which populates excitations lying at relatively high energy transfers, even at low temperatures. This is in contrast to the previous experiment,[25] and the QENS spectrometer therefore measures the neutron energy-loss (anti-Stokes) spectrum at low temperatures up to energy transfers large enough to cover the whole range of lattice frequencies. Three detector banks are mounted on a rotatable table which is moved into different angular settings to cover a wide range of momentum transfers.

The sample was prepared by solidifying 99.997% oxygen gas into a 100 mm high, 6 mm diameter, and 0.5 mm thick aluminum can. A residual pressure of about 10^{-6} mbar was achieved and maintained during all of the sample preparation steps, in order to prevent contamination from nitrogen gas (a problem which affected a good number of the previous neutron diffraction measurements). Condensation into liquid O_2 was achieved, and the sample was left to thermalize for

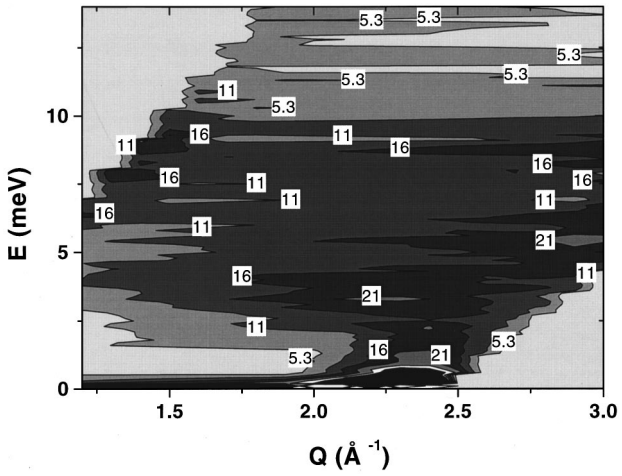

FIG. 2. Contour plot of the total intensities measured for the α phase. The numbers given as insets indicate the relative heights given in arbitrary units. Strong Bragg reflections of magnetic origin were seen at 1.32 and at 1.58 Å^{-1}. Those from the monoclinic lattice appear at 1.68, 2.26, and 2.37 Å^{-1}.

about 30 min. A subsequent drop to 4 K resulted in a polycrystalline α-oxygen sample, the structure of which was ascertained by examination of a time-of-flight diffraction pattern as measured *in situ* with a diffraction detector. The temperature was controlled using two diodes placed just above the sample and at the cold valve, yielding a stability of 0.05 K and a temperature gradient along the sample smaller than 0.1 K. Scans were done at two temperatures within the α phase (4 K and 23 K, 0.9 K below the transition) and at 25 K, not far from the low-temperature limit of the β phase. In all cases the diffraction pattern was inspected repeatedly during the runs, to confirm that no transitions were taking place during the measurements.

Typical counting statistics at $T=4$ K, given in terms of relative errors, were about 17% at an energy transfers of 5 meV and 19% at 10 meV. This is relatively high, due to the weakness of the inelastic signals at such temperatures.

The spectra were treated following the usual procedures for a truly polycrystalline material, which involves the subtraction of scattering from the empty can by means of an attenuation correction, a rough estimate of the importance of multiple scattering effects, and the transformation of spectra from constant angle to constant Q, a step which was achieved by means of a modified version of the INGRID code.[26] The $Z(E)$ frequency distributions were subsequently calculated after performing an angular average over the detector groups, removal of the residual elastic contamination at low frequencies (below 0.15 meV), and extrapolation to zero frequency by a $\propto E^2$ law, estimation of a multiphonon excitation following the procedure described in Ref. 27 and subtraction of this contribution to the total spectrum, and finally, normalization to an absolute scale as discussed below.

A contour plot covering the inelastic region of the energy-loss spectra for the α phase at 4 K is depicted in Fig. 2. As seen there, strong inelastic signals, well separated from the elastic region, appear confined within a region comprising momentum transfers of 1.7 Å^{-1} to 3.0 Å^{-1} and energy-transfers of 2 to 7 meV. A relatively isolated, dispersionless

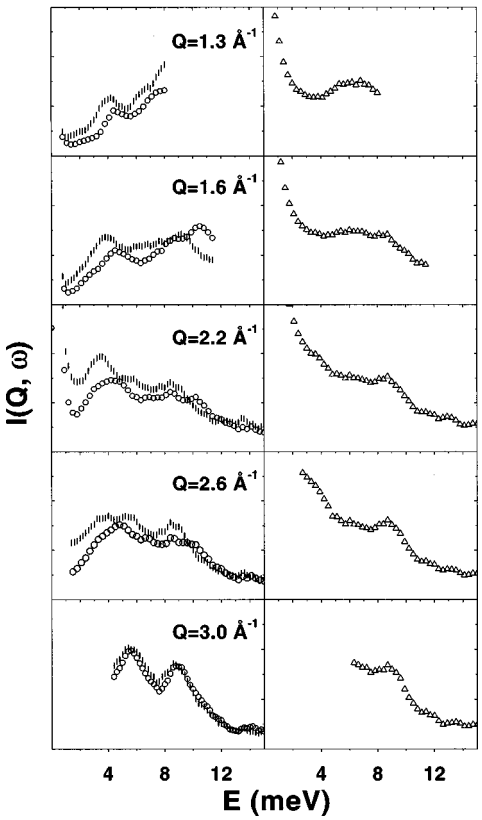

FIG. 3. The left frame of the figure shows experimental spectra for α oxygen at $T=4$ K (circles) and $T=23$ K (vertical bars). The right-hand column displays spectra for the same momentum-transfers (given as insets) for β oxygen at 25 K. All graphs are in the same scale and given in arbitrary units. The curves represent constant-Q spectra derived by interpolation within an smoothed Q-E surface by means of the INGRID code (Ref. 26).-

band appears about 9 meV. The intensities about 8–9 meV and 1.2 Å^{-1} are close to the limits of the kinematically accessible region.

III. RESULTS

A sample of constant-Q spectra corresponding to measurements well within the magnetically ordered domain, and close to the $\alpha \rightarrow \beta$ transition, both within the α-O_2 crystal are shown in Fig. 3. Also shown is the spectrum for the β phase. The plots show that (a) a strong quasielastic component dominates the low frequency spectra (below 6 meV) of the β phase, (b) finite frequency features appear at 8–9 meV above 2 Å^{-1} in spectra for both phases, and (c) an additional feature at lower frequencies (about 4 meV) is only present in the α phase.

The nature of the quasielastic intensities appearing in the magnetically disordered states of O_2 have been discussed in previous papers.[28–30] Such spectral components show a well defined dependence on the wavevector and this was interpreted on the basis of a model for an AF-coupled (i.e., non-ideal) paramagnet, where spin correlations never exceed 6–7 Å. This paramagnetic scattering disappears upon crossing the $\beta \rightarrow \alpha$ transition. Only intensity attributable to the tails of the strong elastic lines is seen at frequencies below 1 meV or so in the α phase. As the results demonstrate, no signature of

quasielastic scattering is visible at 23 K, which is only 0.9 K below the critical $T_{\alpha\rightarrow\beta}$, a temperature at which a substantial reduction (about 40%) in the average value of the magnetic moments has been determined by diffraction.[5]

The finite-frequency feature appearing at 8–9 meV in the spectra of both α and β phases arises from structure-related excitations (phonons). Assignment of a phonon origin to this feature, which is independent of the presence of MLRO, is also supported by the weak dependence of its frequency on wavevector, which goes through a broad maximum at about 1.4 Å^{-1} and shows a shallow minimum at 2.3 Å^{-1}. The latter is clearly visible within the second Brillouin zone (averaged over the different directions), a behavior which conforms to what is expected for an acoustic phonon in a polycrystal.[31] Additional support for such an assignment is provided by the Q dependence of the intensity, which goes through a maximum at Q values close to those corresponding to the lowest Bragg reflection of structural origin (1.68 Å^{-1}).

A peak is also seen at energy transfers about 4 meV in the α phase which disappears upon crossing the transition. It lies on top of a broader feature which was identified as an acoustic phonon in a previous work.[25] Its linewidth is estimated to be of about 1.2 meV at 1.3 Å^{-1} and 4 K and $\approx$1.9 meV at 23 K for the same wave vector, and its integrated intensity is fairly small if compared with that of the phonon background. This makes its Q dependence difficult to track, since both the broad component, whose observation is limited by kinematic effects, and the narrow peak shows a strong angular dependence. The frequency of this feature softens by about 10% when the temperature approaches the phase transformation. The origin of this peak has three plausible origins: a transverse acoustic phonon, an AF magnon (both at the zone boundary), or an admixture of both. The first possibility is inconsistent with the large softening and the lack of a similar feature superimposed on the quasielastic background of the β phase (i.e., the acoustic phonons in both phases are expected to be homologous, given the close structures).

The assignment of a magnetic or magnetovibrational nature to such a low-frequency peak is also supported by the observed softening, which is consistent with a mean-field $\omega_Q \propto (T-T_{\alpha\rightarrow\beta})^{1/2}$ dependence expected for a model such as that examined by LeSar and Etters,[6] where the spin correlations decrease from ideal AF values with rising temperature due to increasing thermal disorder.

A. Frequency distributions

The $Z(E)$ spectral densities of states derived from the present measurements are shown in Fig. 1. The most distinctive features appearing in the distribution for the lower temperature crystal consist of a region of long-wavelength acoustic phonons extending up to about 5 meV, a first peak located at about 5.5 meV, additional structures giving rise to shoulders (or small peaks) at 6–7 meV, an intense and narrow feature peaking at 8.9 meV, and a shoulder at 10.5 meV.

The distributions calculated using the potentials of Jelinek *et al.*[22,23] shown in the inset of Fig. 1 represent a first comparison of calculation and experiment. The main differences are the frequncy range of both distributions in addition to the relative peak intensities. As discussed in the next section, confining the distribution to frequencies below $\approx$10 meV as predicted by the calculation, leads to a large overestimate of the low-temperature specific heat. The experiment and calculation show the same number of extrema. The first two intense peaks in the calculated $Z(E)$ appear at $\approx$5 and 6.5 meV corresponding to the first peak and shoulder of the experimental functions, while the two higher-frequency features seem to have an experimental counterpart in the features at 8.9 and 10.5 meV, which are shifted to higher frequencies by about 0.5 and 1.0 meV, respectively.

As regards the dependence on temperature of the $Z(E)$, the most remarkable findings concern the persistence, even within the β phase of the strong peak at about 9 meV, the strong drop in intensity of the shoulder at 10.5 meV which has nearly disappeared in the β crystal, and the masking of the low frequency ($<$5 meV) spectrum of the β phase. The change in the low frequency region, which is characteristic of long-wavelength phonons, becomes dominated by the strong and broad quasielastic scattering from paramagnons. Softening of the sound velocity is also evident at 23 K, as revealed by the change in curvature of the low-frequency part of the spectra, and the center of gravity of the distribution is shifted to lower frequencies with rising temperature.

The plots shown in the inset of Fig. 1 provide an illustration of the remarkable similarity of the vibrational spectrum on both sides of the $\alpha\rightarrow\beta$ transition. In other words, the lattice distortion accompanying the transition has relatively minor effects in the phonon frequency distributions. The homology of the phonons in the α and β phases has been shown to be fairly independent of the specific kind of potential used in the calculations[22,23,32] and thus it is to be expected that the frequency distributions show the same singularities. Significant deviations from this could then be ascribed either to the presence of features of magnetic origin, or to coupling between structural and spin degrees of freedom. To date, the only unambiguous evidence of such coupling is the large splitting found for the two frequencies of the $Q\rightarrow 0$ collective reorientational motions (i.e., oscillatory motions of the internuclear vector along **a** and **b** crystal axes, referred to as ''librons''), which appear as well defined Raman bands at 5.3 meV (44 cm^{-1}) and 9.8 meV (79 cm^{-1}) in the low-temperature spectrum. The higher frequency mode shows a marked softening as the temperature is raised, reminiscent of the behavior of the magnetic moment[5] and merges with the lower branch[33] after crossing the $\alpha\rightarrow\beta$ transition. Such behavior has here a clear counterpart in the temperature dependence of the 10.5 meV shoulder. Its frequency, which is about 1 meV higher than that found in the Raman spectra, arises from the strong dispersion shown by these modes, a fact accounted for in most of the published calculations.[22,23,32]

B. Thermodynamics

The physical soundness of the measured distributions can be assessed by evaluation of the specific heat at constant volume, performed for temperatures within the range of validity of the quasiharmonic approximation. The result yields $C_V = 0.136(17)\,\text{J mol}^{-1}\,\text{K}^{-1}$ for $T=4$ K, versus an experimental C_P value of 0.116 $\text{J mol}^{-1}\,\text{K}^{-1}$. The comparison cannot sensibly be extended up to $T=23$ K, since a strong in-

crease in anharmonicity (as revealed by a large increase in thermal expansion) is known to take place above 20 K.[34]

The specific heat integral was also evaluated using the experimental density of states for $T=4$ K, as well as that calculated from lattice dynamics for the α phase. The frequency spectra from measurement and calculation were normalized to the number of degrees of freedom deemed relevant at these temperatures $(6R)$. The results are compared as $C(T)/T^3$ with experimental data taken from Fagerstroem and Hollis-Hallet[7] in Fig. 4. This comparison demonstrates that the curve calculated from experimental data has a Debye region [$C(T)/T^3$ independent of temperature] extending up to ≈ 5 K, whereas both the calorimetric results and the curve evaluated from the lattice dynamics distribution confine this regime to temperatures below 1–2 K. Also, both the thermal data and those evaluated from lattice dynamics distribution show a well defined maximum at about 9–11 K which, for the latter, arises from the strong peak in $Z(E)$ at about 5 meV. However, a comparison between thermal measurement and the results from the lattice dynamics distribution shows that the latter far exceed the calorimetric results, indicating that the calculated spectrum is shifted too far towards low frequencies.

Indirect evidence $C_{\mathrm{mag}}(T)$ indicates that there is[2] a contribution of magnetic origin present in the measured specific heat $C_P(T)$. Attempts to estimate such a quantity usually rely on the subtraction of the lattice contribution to the total specific heat $C_{\mathrm{latt}}(T)$ from the measured values. An estimate of such a contribution is given in the review by DeFotis.[2] There, the lattice-phonons contribution to be subtracted is assumed to follow a Debye $C_{\mathrm{latt}}(T)=aT^3$ law within 2 and 8 K. This is at odds with the calculated $Z(E)$ as shown in Fig. 4, but the estimate for $C_{\mathrm{latt}}(T)$ obtained from integrals using the experimental spectrum supports this assumption.

At the temperatures of interest it is expected that most of the heat-carrying spin excitations will be hydrodynamic AF magnons having $\hbar\omega_m$ frequencies close to those signaled by the gaps measured as AFMR resonances, for which $k_BT \approx \hbar\omega_m$. The magnetic contribution to C_P would, in such a limit, be of the form[2]

$$C_{\mathrm{mag}}(T)/T^3=\sum_i A_i\, \mathrm{e}^{-\hbar\omega_i/k_BT}T^{-3/2}, \tag{3}$$

where the sum means that there is more than one AF magnon contributing to this property. To obtain an estimate for $C_{\mathrm{mag}}(T)$, it is assumed that the lattice specific heat can be described by the $C_{\mathrm{latt}}(T)$ calculated using the frequency distribution for $T=4$ K. The difference between experimental specific heat and $C_{\mathrm{latt}}(T)$ is shown in the lower frame of Fig. 4, which comes surprisingly close to the estimate given by DeFotis.[2] Both quantities are found to be of comparable magnitude (about 0.8 $\mathrm{J\,K^{-1}\,mol^{-1}}$ at 10 K, that is about 34% of the total C_P), although they show distinct dependences on temperature.

The result depicted in Fig. 4 shows a Schottky-like maximum, which is consistent with the shape of $C_{\mathrm{mag}}(T)/T^3$ given by Eq. (3). As also shown in the plot, the shape of this curve can be reproduced if a value for $\hbar\omega_i$ midway between the values of the two AFMR frequencies is taken. Hence, the difference $[C_P(T)-C_{\mathrm{latt}}(T)]/T^3$ may be considered as a somewhat more reliable estimate for the magnetic contribution to the heat capacity than those reported to date.

C. Atomic displacement amplitudes

The magnitude of the $\langle u^2\rangle_{\mathrm{av}}^{1/2}$ translational and vibrational displacements in α-O_2 has been estimated from a number of sources.[32,21] The main interest in obtaining reliable estimates for such quantities stems from the effect such motions are expected to exert on the values of the exchange parameters.[11] However, the reported values for $\langle u^2\rangle_{\mathrm{av}}^{1/2}$ are dependent upon the route followed for their estimation, and values as different as 0.25 and 0.092 Å have been reported.[32] The knowledge of the spectral distributions enables the calculation of such parameters by recourse to the approximation[35]

$$\langle u^2\rangle_{\mathrm{av}}=\frac{1}{3MN}\int_0^{E_{\max}} dE\, \coth\left(\frac{\hbar E}{2k_BT}\right)\frac{Z(E,T)}{E}, \tag{4}$$

with M being the molecular mass and N the number of unit cells.[36] The integral is taken over the normalized experimental distributions. Several values for the upper limit $E_{\max}$ are then chosen to explore the contributions to this quantity from different ranges of frequency of $Z(E)$. The values calculated in such a way can be compared with estimates derived from quantum-chemical calculations[21] and optical spectroscopy.[33] At $T=0$ K,[21] the molecules are found to vibrate fairly isotropically with an average amplitude $\langle u^2\rangle_{\mathrm{av}}^{1/2}$ of 0.1032 Å. As regards the molecular librations (i.e., collective reorientations about the crystal *a* and *b* axes), the calculation reports a root-mean-square angular displacement of 11°, which compares well with some previous lattice dynamics and experimental[33] results. The average displacement evaluated from $Z(E,T=4\ \mathrm{K})$ using Eq. (4) and setting $E_{\max}$ to cover the full frequency range yields a value for $\langle u^2\rangle_{\mathrm{av}}^{1/2}$ of 0.164 Å. The difference with the *ab initio* computations can be explained as a finite-temperature effect (the increase in displacement amplitude evaluated by recourse to a Debye approximation[35] gives an increment of 0.0675 Å, yielding a total displacement of 0.1707 Å).

A separation of the translational and librational contributions to these figures can be achieved by inspection of the running integrals of Eq. (4) versus $E_{\max}$. In doing this it was found that long-wavelength acoustic phonons, that is those with energies below 5 meV whose spectrum is accounted by a $Z(E)\propto E^2$ law, contribute about 24% to the total displacements. A rough estimate of the librational amplitude can be made from the contribution to the displacement arising from higher-energy modes. This leads to an average angular displacement of 12°, which nicely matches the calculated values referred to above.

IV. DISCUSSION

The spectra shown in Fig. 3 are consistent with those measured in our previous experiment.[25] Although the available range of energy-transfer was considerably smaller in the previous experiment, a lower angle detector setup enabled the exploration of a region of lower momentum transfers.[25] This provided the wave vector dependence of the low-frequency peak at 4 meV. On the basis of the results, it was

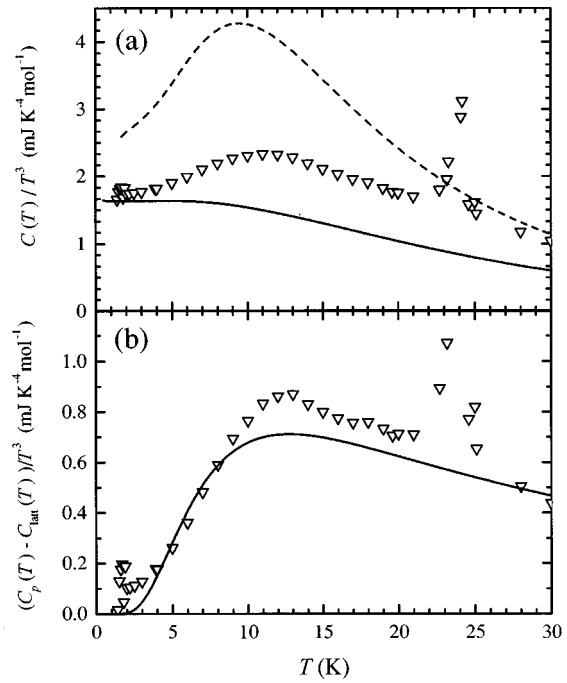

FIG. 4. The upper frame shows a comparison between the experimental heat capacity (triangles) as derived from numerical data given by Fagerstroem and Hollis-Hallet (Ref. 7) and that evaluated from the heat-capacity integral using densities of states $Z(E,T=4$ K) (solid line) and that from the lattice-dynamics calculation (dashes). The lower frame displays the difference $[C_P(T) - C_{\rm latt}(T)]/T^3$ (symbols), where the lattice contribution is approximated by the curve calculated from the experimental frequency distribution and the solid line represents an approximation using Eq. (3) for a energy $\hbar\omega_m = 1.8$ meV (see text).

postulated that the peak contains a strong magnetic contribution.

A. Spectral assignment

As known from studies in a wide variety of molecular crystals,[23] assignment of features of the vibrational frequency distributions to modes with well defined polarizations is usually complicated by the large number of dispersion branches, which contribute with significant intensities at most points within reciprocal space. This leads to peaks in $Z(E)$ having a mixed character (polarization). With such a proviso in mind one can assign a dominant polarization to the three main features of the experimental $Z(E)$, on the basis of the calculated normal mode eigenvectors.[23] The lowest-frequency peak sits at a frequency very close to that of an acoustic mode with mixed polarization ($T_z + T_a$, that is, a translation along the b axis plus a translation perpendicular to the a-b plane, see inset of Fig. 1), as well as with the L_a, lower-frequency ''libron,'' as reported from Raman scattering.[33] The feature at 8.9 meV arises from translational motions with dominant $T_a + T_z$, and T_b polarizations. The shoulder at 10.5 meV can be identified with a zone boundary L_b librational excitation, since its frequency appears in most calculations to be well separated from the rest.[32]

The decrease in intensity of the shoulder observed at 10.5 meV with increasing temperature can thus be attributed to the progressive decrease of the splitting between L_a and L_b modes, which is now understood to arise as a consequence of the coupling of such motions with the long-ranged spin structure. This reduction in frequency will cause such modes to shift towards lower frequencies, and those vibrations will no longer be visible as a well separated feature as the β phase is approached.

The coupling between the spin and lattice degrees of freedom is therefore strong for the librational motions, but becomes far weaker at lower frequencies and especially for temperatures well within the β phase.[28] This is easily understood on the basis of results from first-principles calculations for the α-O_2 crystal,[21] which show that the inclusion of the Heisenberg exchange interaction: (a) lowers the potential energy corresponding to the referred optical vibrations by about 3 meV and (b) splits the otherwise degenerate L_a and L_b modes by an amount which substantially depends upon the deviation of the molecular axes from the normal to the basal planes. In other words, the present result is in agreement with quantum-chemical calculations,[21] which show weak coupling at most of the lattice points, with the exception of those isolated points of the Brillouin zone where the dispersion curves show some avoided crossings.

As far as the strength of such couplings in the β-phase are concerned, their magnitude is expected to be small (if finite). In this respect, it is worth recalling that magnetically it behaves in a way not too different from the rotator crystal or even the liquid.[29,30] The absence of Bragg reflections of magnetic origin implies that no finite-frequency of magnetic origin can sensibly be expected, even if remnants of static short-range order may there coexist with the thermally activated bath of paramagnons.[6,28,37,38]

B. Comparison with previous results

As mentioned in the Introduction, there is a very limited amount of experimental data from other sources to compare with the present results. To the authors knowledge, the only estimates for the vibrational densities of states concern the β phase. A high-pressure (6.0–9.5 GPa) study[39] conducted at room temperature provided the elastic constants, from which the $Z(E)$ were reconstructed employing a lattice-dynamical model. The resulting frequency distributions for an applied pressure of 6.13 GPa show four well resolved bands at about 12, 15.5, 22.7, and 24.8 meV. The peak at 15.5 meV, which is the most intense and narrow feature in the spectrum, is shown to have a large zone-origin libron contribution. The shape of the calculated spectra in Ref. 39 is in general not too different from that of the present measurement, if account is taken of the large pressure-induced shifts and temperature effects which are evident from the large Grüneisen constants reported in that paper.

The kinematic limitations inherent to our experimental setup hinder a detailed comparison with results reported by Stephens *et al.*[16] The narrow feature observed by these authors at about 1.3 Å^{-1} and $\approx$10 meV is outside our available region of Q-E space. If this peak is, as claimed, the only feature of magnetic origin appearing at finite momentum-transfers, then all the intensity appearing in the low E region of the $Z(E)$ spectra would have to be ascribed a lattice origin, which is at odds with the previous discussion. The absence in the spin-flip channel of any clear feature at about 5

meV can be understood on the basis of the moderate resolution in energy transfers (the peak would be substantially contaminated by the elastic line) as well as from the relative weakness of this signal. The sharp features visible in our spectra contrast with the intensity maps for the non-spin-flip channel reported by Stephens *et al.*,[16] which show no clear finite-frequency features (phonons and ''librons'') in the region where such comparison can be made (frequencies of 8–10 meV and wave vectors about 2 Å^{-1} and above). This discrepancy is likely to be a consequence of the statistical accuracy and resolution in energy-transfers achieved in the polarized neutron experiment, which led to a smearing out of the inelastic signals. This is also consistent with the rather different elastic and inelastic intensity ratios found in the two studies.

A possible way out of the apparent dilemma regarding the assignment of the spin excitations can be sought from results obtained from the first-principles, integrated lattice and spin-wave dynamics calculations of Jansen *et al.*[21] If the values calculated in Ref. 21 for the effective coupling parameters are taken, and the assignment of the peak appearing in our spectra at about 1.3 Å^{-1} to a $(0,\frac{1}{2},0)$ zone boundary AF magnon is retained, then the magnon energy at the $b^*/2$ zone boundary turns out to be[15]

$$E_m=(1+\delta\langle S\rangle_0)[8(J_{NNN}-J_\perp-J_{NN})+D], \tag{5}$$

where the symbols retain the same meaning as in Eq. (1). The resulting value for E_m is 4.9 meV (with the spin wave correction set to zero) which is not far from the energy of the lower frequency feature appearing in the present spectra for the α phase. This results from the *ab initio* values of the exchange constants which once averaged over translations and librations yield $J_{NN}=-0.995$ meV, $J_{NNN}=-0.386$ meV, and $J_\perp\approx 0.03$ meV, which are substantially smaller than those estimated previously.[16] However, the parameter set of Ref. 21, while reproducing satisfactorily the AFMR frequencies, cannot reproduce the experimental transverse low-temperature susceptibility [$\chi_\perp=2.4\times10^{-3}$ cm^3/mole (Ref. 2)]. However, the anisotropy parameters provide extra degrees of freedom. For example, Leaving the easy-plane component fixed to its free-molecule value ($D+D'=0.5$ meV), values for the in-plane component ($D-D'=0.028$ meV) and for the spin-deviation ($\delta\langle S\rangle_0=0.223$) can be used. These lead to a value of 5.9 meV for E_m, and they still fulfill the constraint given by Eq. (2). The deviation from the frequency of 4 meV found by experiment is comparable to that found for the higher lying magnon as discussed in the next section. These values yield a susceptibility of $\chi_\perp=3.8\times10^{-3}$ cm^3/mole, which substantially exceeds the experiment. As stated in Ref. 21, such a disagreement may well arise from the mean-field approximation employed to evaluate the susceptibility (a point discussed in more detail in Ref. 21).

The deltalike peak at 10 meV of magnetic origin reported by Stephens *et al.*[16] seems consistent with a higher lying, dispersionless branch of pure magnetic origin also found in the calculations (see Fig. 3 and Table V of Ref. 21), as well as with the frequency of one of the spin excitations of Ref. 38. This interpretation leaves unchanged the basic picture of a quasi-2D model as elaborated by Stephens *et al.*[16] to describe the magnetism of solid oxygen, while modifying the relative strength of the magnetic interactions compared with those of structural (lattice) origin.

The presence of a maximum in the plot of $C_{\text{mag}}(T)/T^3$ shown in Fig. 4 can be interpreted on semiquantitative grounds on the basis of two hydrodynamic AF-magnon frequencies. This, however, is rather simplistic in the light of recent thermal conductivity data,[8] which shows that the description of heat-transport processes in terms of the excitations of a continuum breaks above 5 K. This implies that a more microscopic description of both the phonon and spin-wave spectra are required when a quantitative analysis of the thermodynamics at temperatures about the maxima in C_{mag}/T^3 is attempted. In particular, the effects of magnon-magnon and magnon-phonon interactions need to be quantified.

A way to evaluate the relative importance of nonlinear interactions between the two spin waves, which can easily be operative at temperatures above 5 K, is provided by analysis of the temperature dependence of a property directly proportional to the sublattice magnetization such as data for the magnetic moment.[5] It is then expected that this decrease with temperature should follow[40]

$$\langle M\rangle(T)=M(0)-\left[A\left(\frac{k_{\text{B}}T}{2rJ(T)S}\right)^2+B\left(\frac{k_{\text{B}}T}{2rJ(T)S}\right)^6\right], \tag{6}$$

where A and B are constants readily determined from the geometry of the magnetic lattice, assuming that the interaction with nearest neighbors dominates.[40] Here r is the number of nearest neighbors, and $J(T)$ the exchange constant. The temperature dependence of the coupling constant was set to follow $J(T)=D_0-D_1T^{1/2}$, a formula which accounts for the dependence of values derived from mean-field analyses of the susceptibility.[2,3,11] The value for D_0 was set to that reported above for J_{NN} and D_1 and M_0 were left as adjustable parameters. The plot for $\langle M\rangle(T)$ and its approximation by Eq. (6) is shown in Fig. 5. It corresponds to values of $M(0)=1.43\mu_B$ and $D_1=0.2$ meV $\text{K}^{-1/2}$ and shows that the approximation given by Eq. (6) is able to account for the temperature dependence of the magnetic moment. Evidently the T^6 term, which accounts for the dynamical interaction between the two spin waves, becomes dominant at temperatures above $\approx 10-12$ K.

A test of the consequences of reducing the strengths of the exchange constants with respect to previous estimates,[11,16] is easily performed by calculation of the ordering (Néel) temperature for a two-dimensional system having the same structure than one of the planes of α-oxygen. Moreover, such a system is experimentally accessible, and in fact, a 2D film formed by O_2 molecules physisorbed on graphite has been described[41] and shown to order magnetically at ≈ 12 K. An estimate of the ordering temperature is provided by recourse to the Stanley-Kaplan formula[41,42]

$$T_N=\frac{9}{10}[-2J_{NN}+J_{NNN}]\approx 16 \text{ K}, \tag{7}$$

which still is 4 K above experiment but substantially improves previous estimates.[16]

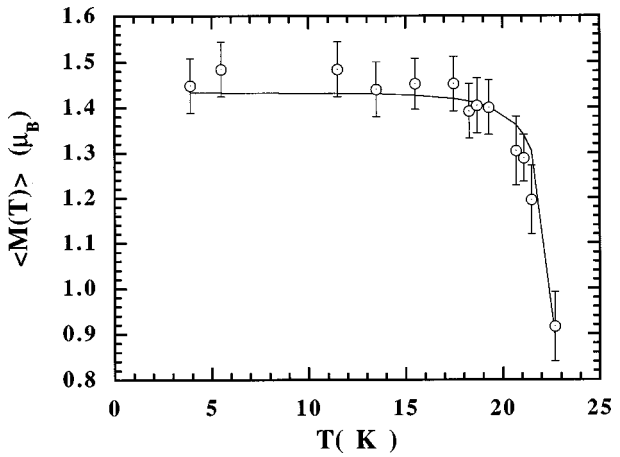

FIG. 5. Temperature dependence of the experimentally determined magnetic moments (symbols) and the approximation given by Eq. (6).

C. A comparison with *ab initio* based results

The agreement between experimental observations and some of the predictions made on the basis of the lattice dynamics–spin-wave formalism described in Ref. 21, suggests that a comparison between calculated quantities and those amenable to measurement is indicated (only dispersion relations are given in Ref. 21). For this purpose, the spectral frequency distributions corresponding to lattice (phonons and librons) and spin excitations (magnons) have been evaluated after a sampling over a grid of $10\times10\times10$ within the irreducible part of the Brillouin zone. The 14 000 states found are separated into those of phonon, libron or magnon character and binned into 0.15 meV bins. The distributions for structure-related and spin-wave excitations are shown in Fig. 6. A comparison between the $Z_{\mathrm{struc}}(E)$ density of states for structural excitations and the experimental spectra shown in Fig. 1 imply that the tentative assignment proposed above should be reassesed. The features within 4–6 meV should have a dominant phonon character with a small contribution from the librons, that found at 9 meV is of mixed (phonon +libron) nature and the shoulder at 10.5 meV is ascribable to librons.

The main differences between calculation and experiment is the disparate ratios of intensities of the different peaks. The discrepancy, although difficult to explain, was not unexpected on the basis of the differences in temperature. As shown in Ref. 39, most of the dominant peaks in $Z(E)$ show large Grüneisen constants. This would not only lead to small peak shifts but will also affect their intensities via changes in the Debye-Waller factors by $2\langle u^2\rangle\gamma\beta T$ where γ stands for the Grüneisen constant and β for the volume coefficient of expansion. A quantitative evaluation of such an effect is hindered by the lack of reliable low temperature data for the two constants.

At any rate, the most relevant finding of such an exercise concerns the spectrum of spin excitations displayed in the lower frame of Fig. 6. As seen there, $Z_{\mathrm{magn}}(E)$ shows two distinct peaks with maxima at about 5 and 12.5 meV. The former has a linewidth of about 0.5 meV whereas the higher-frequency peak has a deltalike character. It seems clear that the spin excitations reported from our experiments and those described by Stephens *et al.*[16] concern the two features

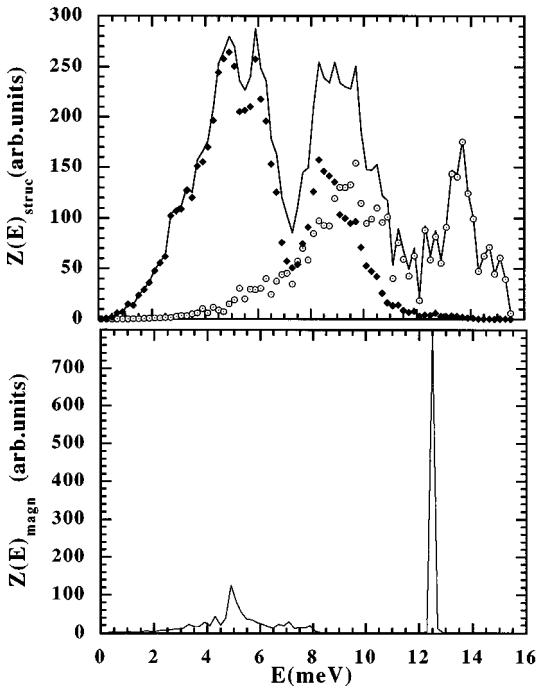

FIG. 6. Calculated density of states for structural (upper frame) and spin (lower frame) excitations in α-O_2. Solid symbols represent the phonon contribution to $Z_{\mathrm{struc}}(E)$ and open circles with a dot stand for the libron modes. The solid line stands for the sum of both contributions.

shown in the figure. The deltalike peak is about 2.5 meV above that published in Ref. 16, although it shows similar characteristics (i.e., strong nondispersive signal), whereas the far less intense peak at about 5 meV comes about 0.5–1.0 meV higher than that observed in the present experiment. The discrepancy can partially be accounted from results given in the previous section. Indeed, Eq. (6) predicts a decrease by $0.2T^{1/2}$ meV of the exchange constant, which should translate into a concomitant frequency softening. Its low intensity means that it will only contribute as a small narrow feature on top of a broad phonon background to the total (unpolarized) spectrum, similar to that shown in Fig. 3. On the other hand, its rather small intensity compared with the higher-frequency peak as well as the difficulty in separating it from the phonon modes, explains why such a feature was not resolved in Ref. 16.

V. CONCLUSIONS

The present results provide a measurement of the spectral distributions of the ordered phases of solid oxygen, for frequencies comprising the lattice motions. Examination of their temperature dependence provides the means to quantify the extent of the coupling between the spin system and the structural degrees of freedom. This comparison shows that the stronger spin-phonon interactions involve collective reorientational motions or ''librons.'' Most of the other vibrations show no measurable signatures of such coupling. The identification of all the spectral features seen as extrema in the frequency distributions for the α phase with vibrational degrees of freedom is also supported by calculation of the specific heat from the measured spectra as well as from the

evaluation o the atomic displacement amplitudes.

Finally, the present measurements have allowed us to reconcile the results of first-principles calculations with experimental findings. Additional details still need to be provided for a complete understanding of the magnetism of this material (especially the determination of the spin-wave stiffness and its temperature dependence), but this has to wait until large single crystals can be grown.

ACKNOWLEDGMENTS

This work was supported in part by DGICYT (Spain) Grant No. PB95-0072-C03-01. The work at A.N.L. was supported by the U.S. Department of Energy, BES-Materials Sciences, under Contract No. W-31-109-ENG-38. Professor Ad van der Avoird is kindly acknowledged for support and stimulating discussions.

[1] H. Kamerling-Onnes and A. Perrier, Leiden Communications **139c**, 25 (1914); A. Perrier and H. Kamerling-Onnes, *ibid.* **139d**, 36 (1914).

[2] G. de Fotis, Phys. Rev. B **23**, 4714 (1981).

[3] R.J. Meier, C.J. Schinkel, and A. de Visser, J. Phys. C **15**, 1015 (1982).

[4] F. Dunstetter, V.P. Plakhti, and J. Schweizer, J. Magn. Magn. Mater. **72**, 258 (1988); R.J. Meier and R.B. Helmholdt, Phys. Rev. B **29**, 1387 (1984); P.W. Stephens, R.J. Birgenau, C.F. Majkrzak, and G. Shirane, *ibid.* **28**, 452 (1983); R.A. Alikhanov, JETP Lett. **5**, 439 (1967).

[5] A. de Bernabé (unpublished); a preliminary account of the behavior with temperature of the magnetic moment as derived from diffraction data is given in F.J. Bermejo *et al.*, J. Low Temp. Phys. **111**, 287 (1998).

[6] Yu.B. Gaididei and V.M. Lotkev, Sov. J. Low Temp. Phys. **7**, 634 (1981); B. Kuchta, T. Luty, and R.J. Meier, J. Phys. C **20**, 585 (1987); R. LeSar and R.D. Etters, Phys. Rev. B **37**, 5364 (1988).

[7] A. Eucken and N. Karwat, Z. Phys. Chem., Stoechiom. Verwandtschaftsl. **112**, 467 (1924); W.F. Giauque and H.L. Johnston, J. Am. Chem. Soc. **51**, 2300 (1929); C.H. Fagerstroem and A.C. Hollis-Hallet, J. Low Temp. Phys. **1**, 3 (1969).

[8] A. Jezowski *et al.*, Phys. Rev. Lett. **71**, 97 (1993).

[9] Yu.A. Freiman *et al.*, Low Temp. Phys. **22**, 194 (1996).

[10] L. Lipinski, A. Szmyrka-Grzebyk, and H. Manuskiewicz, Cryogenics **36**, 921 (1996).

[11] R.J. Meier, Ph.D. thesis, University of Amsterdam, 1984.

[12] I.N. Krupskii, A.I. Prokhvavtilov, Yu.A. Freiman, and A.I. Ehrenburg, Sov. J. Low Temp. Phys. **5**, 130 (1979).

[13] For a comprehensive list of references on infrared, see R.J. Meier, J.H.P. Colpa, and H. Sigg, J. Phys. C **17**, 4501 (1984); Ref. 12; for Raman scattering, see Ref. 33.

[14] E.J. Wachtel and R.G. Wheeler, J. Appl. Phys. **42**, 1581 (1971); T.G. Blocker, M.A. Kinch, and F.G. West, Phys. Rev. Lett. **22**, 853 (1969); Yu.B. Gaididei and V.M. Lotkev, Ukr. Fiz. Zh. **23**, 1147 (1978).

[15] P.A. Lindgaard, R.J. Birgenau, J. Als-Nielsen, and H.J. Guggenheim, J. Phys. C **8**, 1059 (1975).

[16] P.W. Stephens and C.F. Majkrzak, Phys. Rev. B **33**, 1 (1996).

[17] W.J. Briels, A.P.J. Jansen, and A. van der Avoird, *Advances in Quantum Chemistry* (Academic, New York, 1986), Vol. 18, p. 131.

[18] M. Tinkham and M.W.P. Strandberg, Phys. Rev. **97**, 937 (1955).

[19] I.A. Burakhovich *et al.*, JETP Lett. **25**, 32 (1977).

[20] V.A. Slyusarev, Yu.A. Freiman, and R.P. Yankelevich, Sov. J. Low Temp. Phys. **6**, 105 (1980).

[21] A.P.J. Jansen, Ph.D. thesis, Universiteit te Nijmegen, 1987; A.P.J. Jansen and A. van der Avoird, J. Chem. Phys. **86**, 3583 (1987); **86**, 3597 (1987).

[22] G.E. Jelinek, L.J. Slutsky, and A.M. Karo, J. Phys. Chem. Solids **33**, 1279 (1972).

[23] The calculations were performed using the same potential employed for the previous studies on the γ- and β-phases (Refs. 28, 29). A polycrystalline average was taken by dividing the Q space into a fine mesh of $40\times40\times40$ points within the first Brillouin zone. The $Z(E)$ distribution was evaluated by sampling over the Brillouin zone using a mesh of $18\times18\times18$ points along each reciprocal lattice direction.

[24] K.F. Bradley, S-H. Chen, T.O. Brun, R. Kleb, W.A. Loomis, and J.M. Newsam, Nucl. Instrum. Methods Phys. Res. A **270**, 78 (1988).

[25] A. de Bernabé *et al.*, Phys. Rev. B **55**, 11 060 (1997).

[26] The code is a modification for inverted-geometry spectrometers of that developed by F.R. Rieutord, Institut Laue Langevin, France.

[27] J. Dawidowski, R. Fayos, F.J. Bermejo, R. Fernández-Perea, E. Enciso, and S.M. Bennington, Phys. Rev. E **53**, 5079 (1996).

[28] A. Chahid *et al.*, J. Phys.: Condens. Matter **5**, 695 (1993).

[29] A. Chahid *et al.*, Europhys. Lett. **20**, 71 (1992); J. Phys.: Condens. Matter **5**, 423 (1993).

[30] F.J. Bermejo, S. F. J. Cox, M. L. Senent, and J. L. Martínez, Philos. Mag. B **73**, 689 (1996).

[31] F.W. de Wette and A. Rahman, Phys. Rev. **176**, 784 (1968).

[32] R.D. Etters, A.A. Helmy, and K. Kobashi, Phys. Rev. B **28**, 2166 (1983); A. Helmy, K. Kobashi, and R.D. Etters, J. Chem. Phys. **80**, 2782 (1984).

[33] R.J. Meier, M.P. Van Albada, and A. Lagendijk, Phys. Rev. Lett. **52**, 1045 (1984); K.D. Bier and H.J. Jodl in *Dynamics of Molecular Crystals*, edited by J. Lascombe (Elsevier, Amsterdam, 1987), p. 453.

[34] V.G. Manzhelii, A.M. Tolkachev, and E.I. Voitovich, Phys. Status Solidi **13**, 351 (1966); R.J. Stevenson, J. Chem. Phys. **27**, 673 (1957).

[35] S.W. Lovesey, *Theory of Neutron Scattering from Condensed Matter* (Clarendon, Oxford, 1996), Vol. 1, Chap. 9, p. 113.

[36] B.T.M. Willis and A.W. Pryor, *Thermal Vibrations in Crystallography* (Cambridge University Press, Cambridge, 1975), p. 81. The quantity calculated from $Z(E)$ should be taken as an average over all directions. Some of the displacements along the crystal axes are substantially larger, as shown in Table 3 of Ref. 21.

[37] F. Dunstetter, Ph.D. thesis, Université de Paris-Sud, 1988.

[38] A.J.R. da Silva and L.M. Falicov, Phys. Rev. B **52**, 2325 (1996).
[39] E.H. Abramson, L.J. Slutsky, and J.M. Brown, J. Chem. Phys. **100**, 4518 (1994).
[40] S.W. Lovesey, *Theory of Neutron Scattering from Condensed Matter* (Clarendon, Oxford, 1996), Vol. 2, Chap. 9, p. 123.
[41] P.W. Stephens *et al.*, Phys. Rev. Lett. **45**, 1959 (1980); M. Nielsen and J.P. McTague, Phys. Rev. B **19**, 3096 (1979).
[42] H.E. Stanley and T. Kaplan, Phys. Rev. Lett. **17**, 913 (1966).